Pergamon

Bioorganic & Medicinal Chemistry 6 (1998) 1745–1757

BIOORGANIC & MEDICINAL CHEMISTRY

Molecular Structure and Stereoelectronic Properties of Sarmazenil—a Weak Inverse Agonist at the Omega Modulatory Sites (Benzodiazepine Receptors): Comparison with Bretazenil and Flumazenil

B. López-Romero,[a,*] G. Evrard,[a] F. Durant,[a] M. Sevrin[b] and P. George[b]

[a]*Laboratoire de Chimie Moléculaire Structurale, Facultés Universitaires Notre-Dame de la Paix, rue de Bruxelles 61, B-5000 Namur, Belgium*

[b]*Synthélabo Recherche (L.E.R.S), Ave. Paul Vaillant Couturier 31, F-92220 Bagneux, France*

Received 12 December 1997; accepted 1 May 1998

Abstract—X-ray diffraction and ab initio MO theoretical calculations were used in order to investigate the structural and electronic properties of sarmazenil, a weak inverse agonist at the ω modulatory sites (benzodiazepine receptors). This compound was compared to bretazenil, a partial agonist, and to the antagonist flumazenil on the basis of structural and electronic data. The conformational and theoretical properties (interatomic π overlap populations, molecular electrostatic potential (MEP), the topology of frontier orbitals, and proton affinity) of these three imidazobenzodiazepinones were determined in order to analyse the stereoelectronic properties in relation with their distinct intrinsic efficacies at the ω modulatory sites.

Introduction

Benzodiazepines are among the most widely used drugs in the treatment of anxiety and sleep disorders as a consequence of their broad spectrum of anxiolytic, hypnotic, anticonvulsant, and muscle relaxant properties.[1,2] They exert their therapeutic effects by acting at the ω modulatory sites (BZ receptors), which are allosteric sites located at the macromolecular $GABA_A$ receptor complex and regulate the chloride ion flux within the associated ion channel.[3–5] The $GABA_A$ receptor complex is formed by the combination of distinct subunits, which are named α, β, γ, δ, and ρ based on their amino-acids sequence homology. The exact subunit composition/stoechiometry is not known at this time but a pentameric model of the ligand-gated ion channel complex in which each subunit has four membrane-spanning domains has been proposed.[6] For most of these subunits, several isoforms have been described and cloned.[7–18] These ω modulatory sites have been classified into two pharmacologically different subtypes, ω_1 (BZ_1) and ω_2 (BZ_2),[19,20] on the basis of their different affinities for the triazolopyridazine, Cl 218,872, the imidazopyridine, zolpidem, and some β-carboline derivatives. Each subtype presents a distinct distribution in the central nervous system.[20–25]

Ligands acting at the ω modulatory sites (Fig. 1) can differ by their intrinsic efficacy.[26] At least, three classes of compounds have been identified based on their ability to modulate GABA neurotransmission by interacting with this receptor complex. Positive modulation, which leads to a potentiation of the GABA-induced chloride ion flux, is produced by agonists at the ω modulatory sites, such as benzodiazepines (e.g. flunitrazepam,[26] diazepam,[26] oxazepam,[26] midazolam,[27] and triazolam[27]), cyclopyrrolones (e.g. zopiclone[26,28] and suriclone[28]), triazolopyridazines (e.g. Cl 218,872[27]), imidazopyridines (e.g. zolpidem[29]), β-carbolines (e.g. ZK 91296[30]), and imidazopyrimidines.[31] Negative modulation, which induces a decrease of the GABA-induced chloride ion flux, is obtained by inverse agonists, such as β-carbolines (e.g. β-CCM[26,30] and DMCM[26,30,32]),

Key words: X-ray diffraction; MO calculations; ω modulatory sites; partial agonist; flumazenil; sarmazenil; bretazenil.

*Corresponding author. Tel: 32 81 72 45 55; Fax: 32 81 72 45 30.

0968-0896/98/$—see front matter
PII: S0968-0896(98)00117-5

pyrazoloquinolines (e.g. CGS 8216[33]), whereas competitive antagonists of the ω modulatory sites (such as the benzodiazepine flumazenil,[34] the β-carbolines ZK 93426,[35] PrCC,[36] and β-CCt[37]) bind without intrinsic activity.

The aim of this work is to determine the structural and electronic properties responsible for the intrinsic activity of distinct prototype compounds from the imidazobenzodiazepinone series.

In order to analyse the stereoelectronic properties potentially related to the intrinsic activity of antagonists and partial agonists at ω_1 modulatory sites, we focused our study on bretazenil, sarmazenil and flumazenil (Fig. 2) for several reasons. Belonging to the same chemical series, the imidazobenzodiazepinones, the structural and electronic properties divergences caused by a structural heterogeneity are limited. Secondly, these molecules possess similar binding profiles and affinities at the $\alpha_x\beta_2\gamma_2$ recombinant receptors[38] and for ω_1 modulatory sites.[39] They differ in terms of their intrinsic efficacies: antagonism for flumazenil,[34] partial agonism for bretazenil,[40] and sarmazenil, formerly described as an antagonist and later identified as a weak inverse agonist.[41–44]

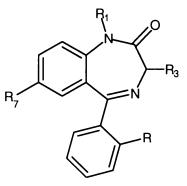

flunitrazepam: $R_7 = NO_2$, R_1 = Me, R = F
diazepam: R_7 = Cl, R_1 = Me
oxazepam: R_7 = Cl, R_1 = H, R_3 = OH

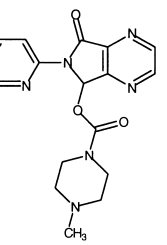

zopiclone

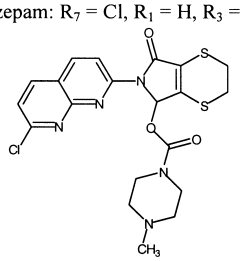

suriclone

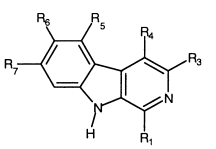

β-CCM: R_3 = COOMe
β-CCt: R_3 = COO-*t*-But
DMCM: R_3 = COOMe, R_4 = Et, R_6 = R_7 = OMe
ZK93426: R_3 = COOEt, R_4 = Me, R_5 = O-*i*-Pr
PrCC: R_3 = COO-*n*-Pr
ZK91296: R_3 = COOEt, R_4 = CH_2OMe, R_5 = OCH_2Ph

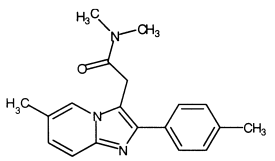

zolpidem

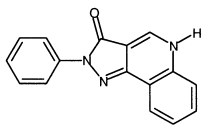

CGS 8216

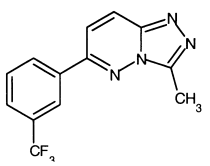

Cl 218,872

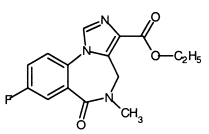

flumazenil

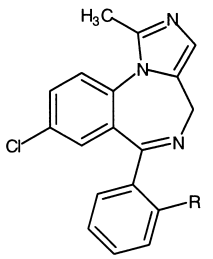

midazolam: R = F
triazolam: R = Cl

Figure 1. Chemical structures of some ω modulatory sites ligands.

In the present work, the X-ray structures of the three molecules are compared and ab initio molecular orbital (MO) calculations using the X-ray structures are performed in order to obtain information about the electronic descriptors, which characterize the partial agonist, the inverse agonist, and the antagonist properties. The electronic descriptors studied are interatomic π overlap populations, molecular electrostatic potential (MEP), topology of frontier orbitals, and proton affinity.

Results and Discussion

X-ray results

All crystallographic data for sarmazenil are reported in Table 1. The atom numbering, bond lengths, and valence angles are presented in Figure 3. Final atomic parameters and thermal factors are listed in Table 2. Figure 4 presents the stereoscopic view of the molecular conformation with vibration ellipsoids (50% of probability). The crystal packing (Fig. 5) is mainly due to van-der-Waals interactions. However, it can be seen that the ester carbonyl from one sarmazenil molecule lies over the phenyl ring from another molecule at a mean distance of 3.8 Å, suggesting a π–π interaction between these two entities.

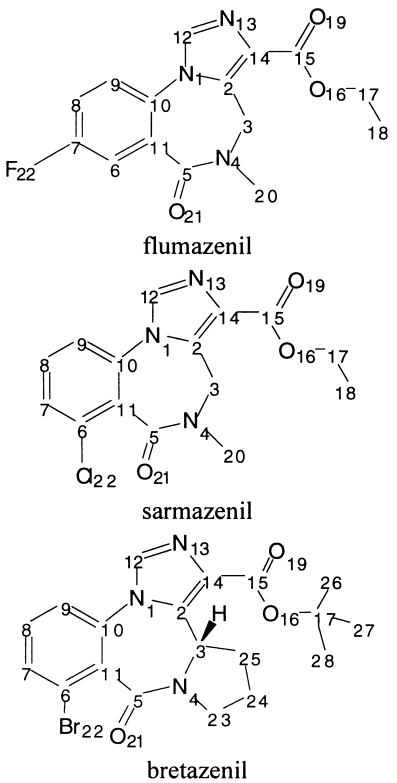

Figure 2. Chemical structures and atom numbering of flumazenil, sarmazenil, and bretazenil.

The main dihedral angle values of sarmazenil are summarized in Table 3 and are compared to those of bretazenil and flumazenil, whose crystallographic coordinates have been obtained from the Cambridge Structural Database (CSD).[45] The dihedral angles between the phenyl ring and the lactame function (C_6–C_{11}–C_5–O_{21}) and between the phenyl and imidazole rings (C_9–C_{10}–N_1–C_2) are very similar for the three compounds. On the other hand, the dihedral angle between the imidazole ring and the ester function (C_2–C_{14}–C_{15}–O_{19}) is significantly higher for bretazenil (140.0°) than for the two other molecules (−165.0° and −162.4° for flumazenil and sarmazenil, respectively), due to a steric interaction caused by the presence of the saturated ring fused at position 3–4. This geometric particularity is illustrated in Figure 6, where the three compounds are superimposed. In order to verify if the steric properties of the molecules could be in relation with their intrinsic efficacies, a conformational analysis was performed.

Theoretical conformational analysis

Starting from the crystallographic data, we performed semiempirical MO AM1 calculations in order to scan

Table 1. Crystal data, data collection, and structure refinements of sarmazenil

Molecular formula	$C_{15}H_{14}ClN_3O$
Molecular mass	319.7
Crystal system	Tetragonal
Space group	$P4_2/n$
a (Å)	19.2977 (10)
b (Å)	19.2977 (10)
c (Å)	8.1773 (10)
V (Å^3)	3045.2 (4)
Z	8
D_x (g cm^{-3})	1.395
Temperature (K)	293
Crystal dimensions (mm)	0.35×0.18×0.17
Radiation	Graphite monochromated CuK_α ($\lambda = 1.54178$Å)
Diffractometer	Enraf–Nonius CAD-4
Absorption coefficient (cm^{-1})	23.7
F (000)	1328
2θ range (°)	6.4–143.8
Unique data	2986
Unique data with $F_0 \geq 4.0\,s(F_o)$	1536
R final	0.05
wR^2 final	0.17 with $w = 1.0/(s^2(F^2) + (0.0943P)^2 + 0.00P)$ $P = (Max(F_o^2,0) + 2F_c^2)/3$
Max and min heights in final D-Fourier (e-Å^3)	−0.25 and 0.31
$(D/s)_{max}$	0.12

the conformational space of the ester chain. Figure 7 represents the energetic variations due to the modification of the ester chain orientation by rotation around the T_1 and T_2 torsion angles of sarmazenil and bretazenil. The two-dimensional isoenergy contour maps clearly show a unique energetic minimum for each compound corresponding to the crystallographic conformation. However, the energetic minimum of bretazenil is shifted by 60° in comparison with sarmazenil. This difference is due to the steric hindrance of the *t*-butyl ester side chain moiety, which orientates the ester carbonyl group differently for bretazenil (Fig. 6). For sarmazenil the dihedral angle value between the planes of the imidazole ring and the ester function is +20° (above the imidazole plane), whereas a dihedral angle of −45° (under this plane) prevails for bretazenil.

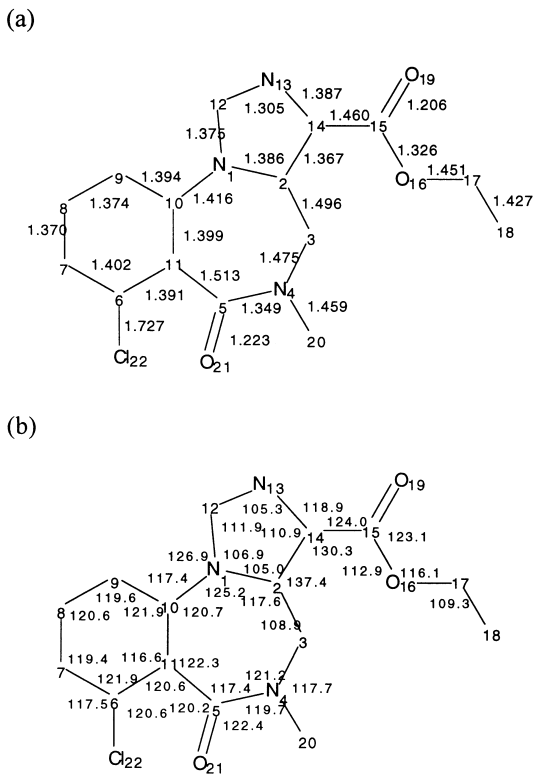

Figure 3. Bond lengths (Å) and valence angles (°) of sarmazenil (a) and (b). Max. standards of error are 0.005 Å and 0.8°, respectively.

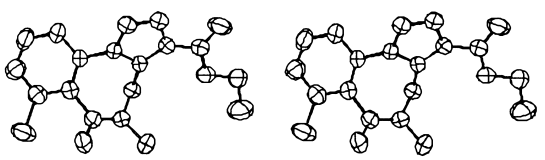

Figure 4. Stereoscopic view of the molecular conformation of sarmazenil with vibration ellipsoids (50% of probability).

A comparable conformational analysis was performed for the structurally related molecule Ro 15-4941, which displays an antagonistic activity.[46] This molecule possesses the same structure as sarmazenil with a five-membered ring fused at position 3–4. The isoenergy map obtained (Fig. 7) shows a similar pattern as that of sarmazenil. However, two energy minima are pointed out for this compound, which corresponds to dihedral angle values between the imidazole ring and the ester function equivalent to +60° (above the imidazole plane) and −15° (under this plane), respectively. A common ester function conformation is observed for the antagonists/inverse agonists which corresponds to a mean dihedral angle value of +40° (±20°) above the imidazole plane. This conformation could lead to the antagonistic/inverse agonistic activity. In the case of bretazenil, a dihedral angle value of −45° (under the imidazole plane) is observed. Given that the antagonist Ro 15-4941 shows one ester conformation similar to bretazenil,

Table 2. Fractional atomic coordinates (10^4) and U_{eq} of sarmazenil[a]

Atoms	x/a	y/b	z/b	U_{eq}
N(1)	8622(1)	1734(1)	8101(3)	56(1)
C(2)	8389(1)	1137(1)	7332(4)	52(1)
C(3)	8864(1)	800(2)	6124(4)	58(1)
N(4)	9490(1)	558(1)	6984(4)	60(1)
C(5)	9949(2)	1010(2)	7625(4)	62(1)
C(6)	10385(2)	2183(2)	6732(5)	71(1)
C(7)	10325(2)	2906(2)	6611(5)	79(1)
C(8)	9719(2)	3221(2)	7066(5)	78(1)
C(9)	9162(2)	2833(2)	7572(4)	66(1)
C(10)	9220(2)	2113(2)	7653(4)	56(1)
C(11)	9838(2)	1771(2)	7266(4)	57(1)
C(12)	8102(2)	1946(2)	9137(4)	64(1)
N(13)	7566(1)	1536(1)	9072(4)	66(1)
C(14)	7740(2)	1027(2)	7946(4)	56(1)
C(15)	7238(2)	481(2)	7590(4)	62(1)
O(16)	7520(1)	−60(1)	6842(3)	73(1)
C(17)	7054(2)	−628(2)	6463(5)	83(1)
C(18)	7449(2)	−1218(2)	5972(7)	127(2)
O(19)	6630(1)	517(1)	7912(4)	93(1)
C(20)	9524(2)	−172(2)	7441(5)	83(1)
O(21)	10439(1)	824(1)	8466(3)	78(1)
CL(22)	11161(1)	1814(1)	6144(2)	104(1)

[a] U_{eq} is defined as one-third of the trace of the orthogonalized U_{ij} tensor.

Table 3. Values of the main dihedral angles of flumazenil, sarmazenil, and bretazenil

Dihedral angle (°)	Flumazenil	Sarmazenil	Bretazenil
C_6–C_{11}–C_5–O_{21}	34.6	48.0	48.0
C_9–C_{10}–N_1–C_2	141.1	135.1	129.9
C_2–C_{14}–C_{15}–O_{19}	−165.0	−162.4	140.0

but the angle value being −15°, one can assume that the agonistic activity can be related to an ester conformation within a dihedral angle between −15° up to −45°. Thus, from a conformational point of view, a hypothesis allows to explain the intrinsic activities of these molecules. The possibility of distinct binding modes in the same active site at the ω modulatory sites leading to differing intrinsic efficacies could therefore be considered.

Ab initio molecular orbital calculations

The electronic properties were calculated for flumazenil, bretazenil, and sarmazenil, from the single-crystal X-ray coordinates for the heavy atoms. The calculations were performed according to the ab initio MO–LCAO–SCF method using a STO-3G* basis set.

(a) The interatomic π-overlap populations (Fig. 8), calculated according to the Mulliken charge population analysis, show an electronic delocalization within the phenyl and the imidazole rings. No significant conjugation exists between the former ring and the lactam function and the latter ring with the ester function. These observations confirm the crystallographic data observed for sarmazenil, for which the bond lengths (C_5–C_{11} = 1.513 Å, C_{10}–N_1 = 1.416 Å and C_{14}–C_{15} = 1.460 Å) are characteristic of single bonds. The dihedral angle values (Table 3) between the phenyl and imidazole rings, between the phenyl ring and the lactam function and between the imidazole ring and the ester function show that these moieties are not coplanar and do not allow electron delocalization.

(b) The molecular electrostatic potential (MEP) were considered as another parameter of interest. It represents the electrostatic forces displayed by a ligand when it interacts with the receptor. Three-dimensional MEP plots were calculated (Fig. 9). The negative equipotential surfaces drawn describe attractive interaction energies for a proton and thus simulating a protonic receptor site. For each compound we observe three proton acceptor sites generated by the imidazole N_{13} atom (−92.5 kcal/mol), the ester carbonyl O_{19} atom (−65.0, −66.0, and −72.0 kcal/mol for flumazenil, sarmazenil, and bretazenil, respectively) and the lactam carbonyl O_{21} atom (−54.0, −59.5, and −63.5 kcal/mol for flumazenil, sarmazenil, and bretazenil, respectively). It can be considered that the general MEP pattern of the three molecules is similar. Three proton acceptor sites are pointed out, which can be considered as potential binding sites to the ω_1 modulatory site.

(c) Energy and topology of frontier orbitals. π–π interactions or charge transfer are considered as an important mode of interaction between a ligand and a receptor. Therefore, it is of interest to calculate the energy and to visualize the topology of the highest occupied and the lowest unoccupied orbitals (HOMO and LUMO,

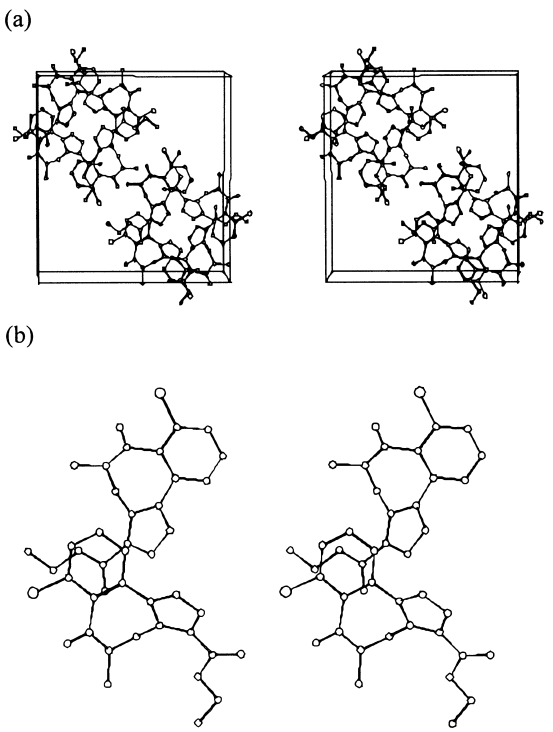

Figure 5. Stereoscopic view of the crystal packing of sarmazenil (a) showing π–π interactions between sarmazenil molecules (b).

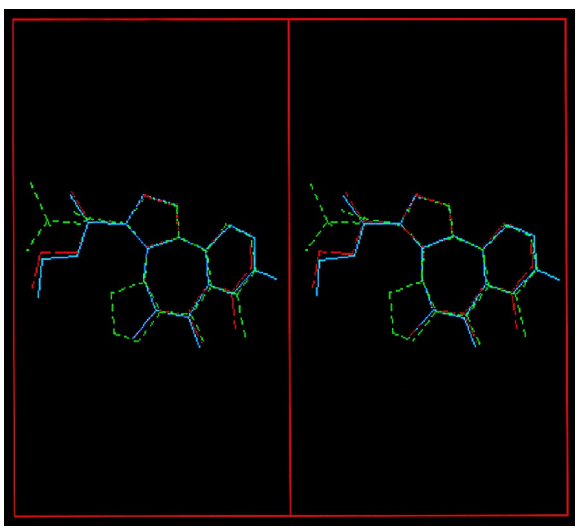

Figure 6. Stereoscopic view of the superimposition of flumazenil (blue), sarmazenil (red), and bretazenil (green).

respectively). To fulfil this study, the molecules were oriented in the xz plane of the imidazole and phenyl rings, as well as in the plane of the ester function. The $2p_y$ atomic orbitals, perpendicular to the molecular plane, then contribute to the electron density, which could be implicated in charge transfer interactions.

The topologies of the HOMOs, centered on the imidazole ring, and the LUMOs, centered on the phenyl ring, are very similar to each other as shown in Figure 10. In the case of a π–π type interaction with the receptor, the imidazole ring would act as an electron donor, whereas, the phenyl ring would play an electron acceptor role. Moreover, the carbonyl of the ester function also contributes to the HOMO (Fig. 11) and therefore this group could act as electron donor in a charge transfer process, as observed in the crystal packing of sarmazenil.

The energy levels of the frontier orbitals are summarized in Table 4 and show no significant differences between the three compounds for the HOMOs and LUMOs values. These parameters do not discriminate between partial agonist, inverse agonist, and antagonist properties. However, Schove and co-workers[47] have proposed a model of ω ligands/receptor interactions and have hypothesized that activation of the ω mod-

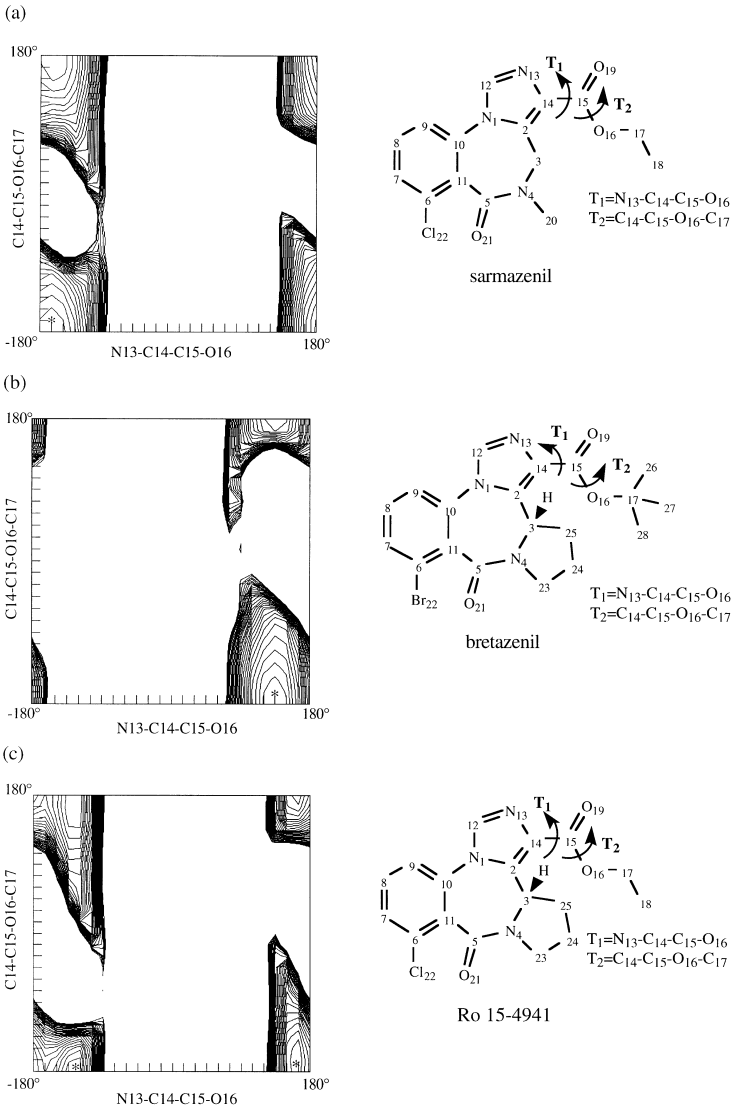

Figure 7. AM1 isoenergy contour map (k_{cal}/mol) for (a) sarmazenil, (b) bretazenil, and (c) Ro 15-4941. The contour-to-contour interval is 1 k_{cal}/mol. The asterisk indicates the energy minimum.

ulatory sites would occur through a charge transfer interaction between an electron accepting ring of the ligand and an electron donating ring in the receptor. This study concerns molecules belonging to different chemical series, only one molecule representing each series. The position of the electron accepting ring is considered as a discriminant property for agonism, inverse agonism, and antagonism. Our studies show that MEP and frontier orbitals of the three superimposed imidazobenzodiazepinones, the partial agonist, the inverse agonist, and the antagonist, fit with a three-proton-acceptor sites model and orientate the LUMOs in the same spatial region. Therefore, in contrast to the Schove hypothesis, LUMOs cannot be taken as an argument for activity discrimination. However, the Schove study could lead to different conclusions for two reasons. Firstly, in the same chemical series the molecules could present different intrinsic activities (our case). Secondly, the selection of a high number of structurally different compounds does not take into account the possibility of different interaction sites between chemical series.

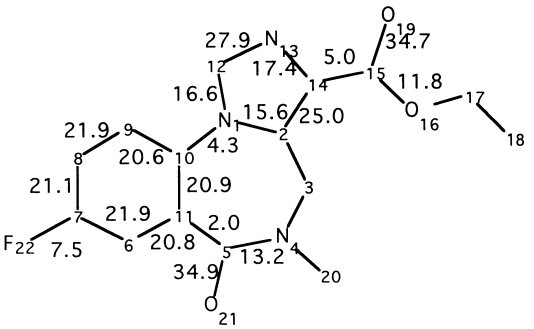

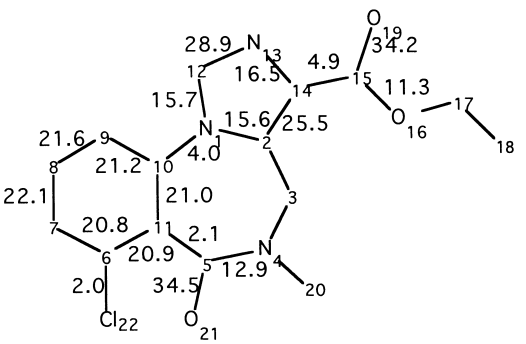

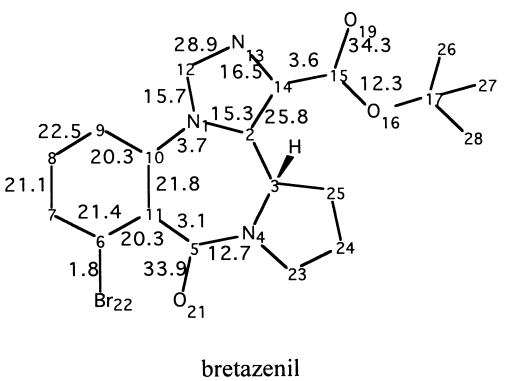

Figure 8. Interatomic π-overlap populations (%) of flumazenil, sarmazenil and bretazenil based on ab initio MO STO-3G* Mulliken population analysis.

(d) Proton affinities are a theoretical measure of the basicity of a specific site of the molecule. They were calculated as the energy difference between the protonated and non-protonated form[48–50] of each electronic lone pair of the proton acceptor atoms of the molecules after a geometrical optimization and are listed in Table 5. The greater the energy difference, the greater is the proton affinity. For the three compounds, the O_{19} atom of the ester chain appears to possess the greater proton acceptor property, followed by the imidazole N_{13} atom and the O_{21} atom of the lactam function. In general, differences in proton affinities are found between the two electron lone pairs of the ester O_{19} atom and the lactam O_{21} atom, depending on their orientation. Proton affinities are stronger for the O_{19} lone pairs oriented towards the N_{13} atom (2 versus 1). For sarmazenil and bretazenil, but not for flumazenil, proton affinities are stronger for the O_{21} lone pairs oriented towards the halogen atoms (4 versus 3). For flumazenil, the F_{22} atom exerts less influence on the proton affinity of the O_{21} atom in regard to its two lone pairs, due to its position on the phenyl ring.

Two main structural differences between the three compounds are pointed out. The first is the halogen atom on the phenyl ring: on position 6 for both the partial agonist and the inverse agonist and on position 7 for the antagonist. The second concerns the ester side chain: a *t*-butyl for the agonist and an ethyl for both the antagonist

Table 4. Energy of frontier orbitals HOMO and LUMO of flumazenil, sarmazenil, and bretazenil

Energy (k_{cal}/mol)	Flumazenil	Sarmazenil	Bretazenil
HOMO	−165.363	−167.975	−167.868
LUMO	126.715	126.370	127.418

and the inverse agonist. Therefore, the difference in intrinsic efficacy could be considered as a consequence of the changes in the substitution on the phenyl ring and/or the ester side chain, which could have repercussions on the proton affinity values of O_{21} and O_{19} atoms, respectively. The three-dimensional (3-D) MEP maps (Fig. 9) calculated from the electronic density were subsequently analyzed to find the lowest electrostatic potential minimum close to the lactam oxygen [$E_{min}(O_{21})$] and the ester oxygen [$E_{min}(O_{19})$]. The depths of the minima found, which have been correlated with O_{21} and O_{19} atom's ability to accept a proton in a hydrogen bond, decrease in the following order for [$E_{min}(O_{21})$]: bretazenil (−63.5 kcal/mol) > sarmazenil (−59.5 kcal/mol) > flumazenil (−54.0 kcal/mol). The [$E_{min}(O_{19})$] decreases as follows: bretazenil (−72.0 kcal/mol) > sarmazenil (−66.0 kcal/mol) ≥ flumazenil (−65.0 kcal/mol). The lower [$E_{min}(O_{21})$] and [$E_{min}(O_{19})$], the more attractive towards a proton the atom is considered.

Further to our results, it can be advanced that the ability of a compound to attract a proton would be in relation with its agonist properties and could represent a positive allosteric effect at

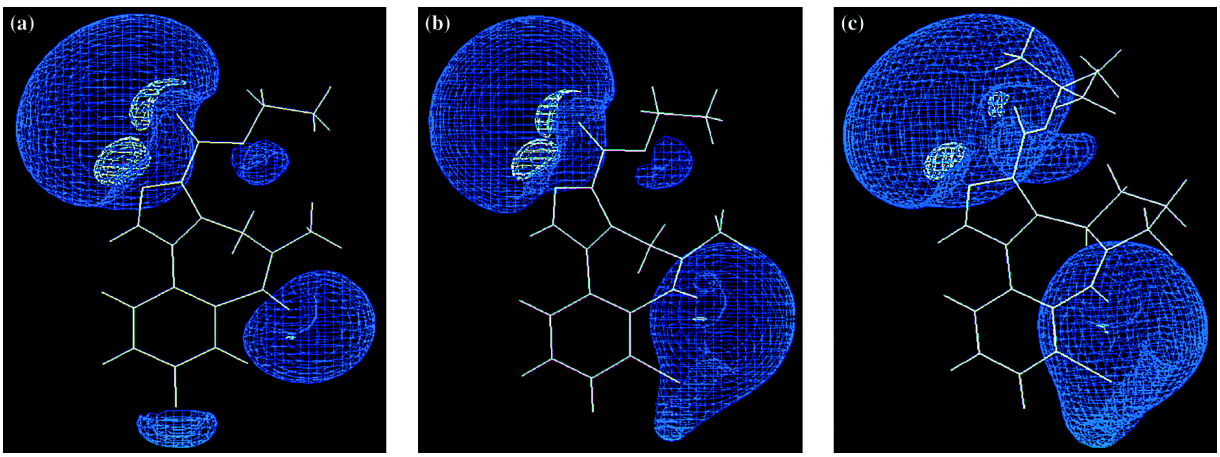

Figure 9. Three-dimensional molecular electrostatic potential isoenergy surfaces. (a) Flumazenil: red = −92.5 kcal/mol; white = −54.0 kcal/mol; blue = −10.0 kcal/mol. (b) Sarmazenil: red = −92.5 kcal/mol; white = −59.5 kcal/mol; blue = −10.0 kcal/mol. (c) Bretazenil: red = −92.5 kcal/mol; white = −63.5 kcal/mol; blue = −10.0 kcal/mol.

Table 5. Proton affinities at different sites of flumazenil, sarmazenil, and bretazenil

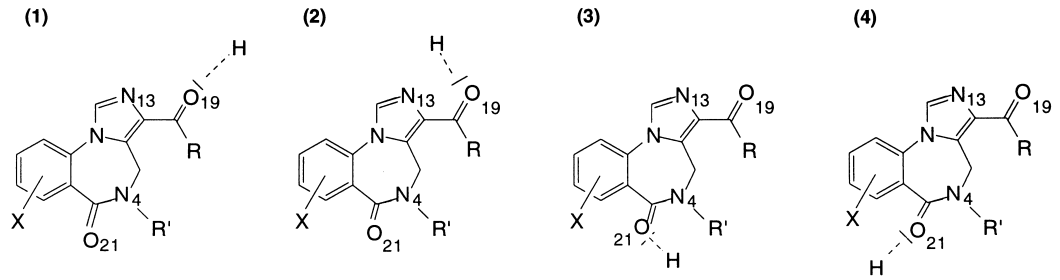

Proton affinity (k_{cal}/mol)	Flumazenil	Sarmazenil	Bretazenil
N_{13}	291.8	292.3	297.7
O_{19}(1)	279.3	284.9	287.8
O_{19}(2)	293.0	298.5	306.7
O_{21}(3)	285.4	282.1	296.6
O_{21}(4)	288.6	288.0	302.9

the $GABA_A$ receptor complex. On this basis, it is possible to differentiate bretazenil from flumazenil (agonism from antagonism). However, weak negative modulation of sarmazenil observed in vivo is not detected through this electronic parameter. The calculated attractive energy of sarmazenil could be correlated to a weaker activity than partial agonism (i.e. close to the antagonist activity).

In addition to that, some structurally related molecules[46] clearly show that the ester side chain could be considered as responsible of the intrinsic activity of the imidazobenzodiazepinones at the ω modulatory site. Molecules such as Ro 16-0075 and Ro 16-3774, which carry a chlorine atom and a methyl substituent at position 6 of the phenyl ring, respectively, and a *t*-butyl ester side chain, have the same intrinsic activity as bretazenil. The Ro 15-4941 compound differs from Ro 16-0075 by an ethyl ester instead of a *t*-butyl ester function, it displays antagonist/inverse agonist activity.

Thus, we have shown in the conformational analysis that the major element governing the intrinsic activity of these molecules could be the ester function conformation, which is related to its alkyl chain. Compared to the previous physico-chemical parameters studied, the ester function proton affinity calculations allow to

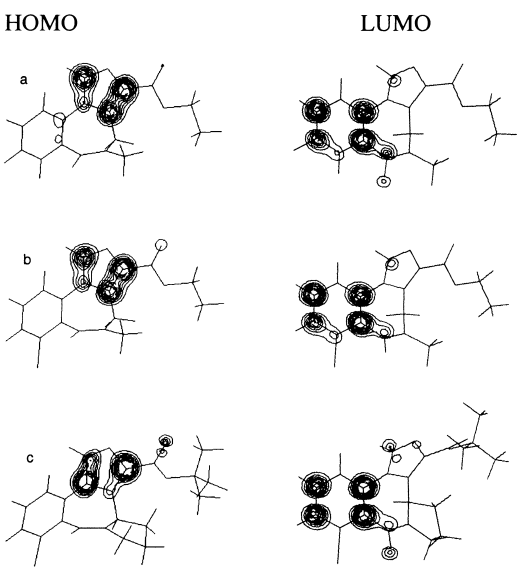

Figure 10. Topologies of HOMO and LUMO of (a) flumazenil, (b) sarmazenil, and (c) bretazenil with molecules orientated in the xz plane of the imidazole and phenyl rings: the isoelectron density contours from 0.005 to 0.025 $e^-/Å^3$ in dotted lines and from 0.030 to 0.050 $e^-/Å^3$ in solid lines.

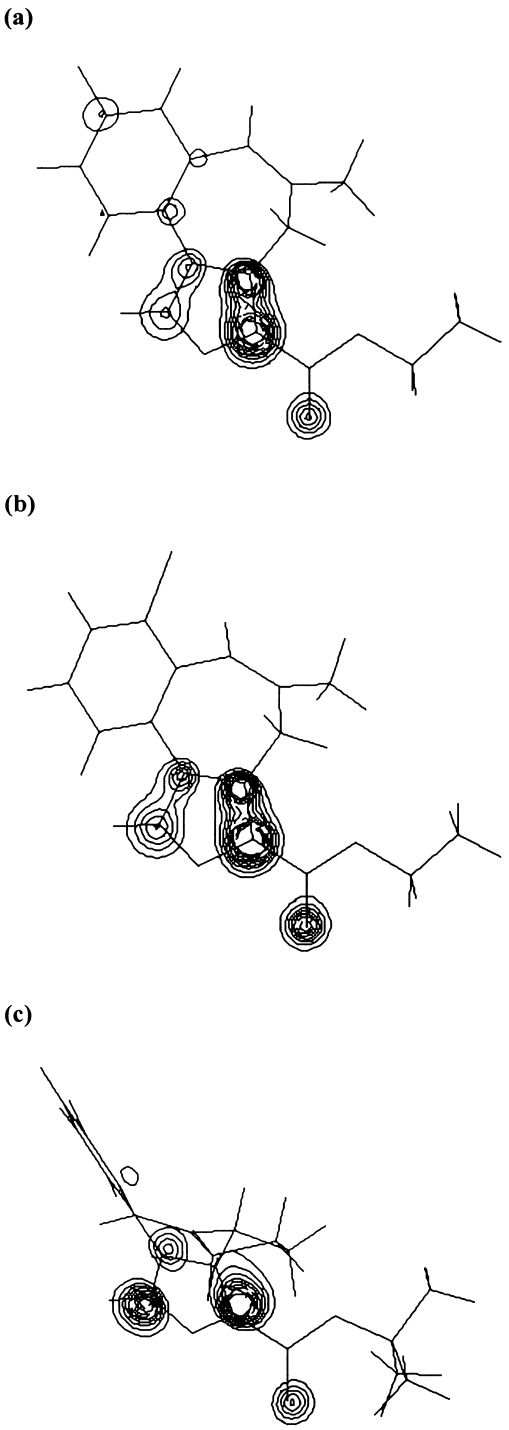

Figure 11. Topologies of HOMO of (a) flumazenil, (b) sarmazenil, and (c) bretazenil with molecules oriented in the xz plane of the ester function: the isoelectron density contours from 0.005 to 0.025 $e^-/Å^3$ in dotted lines and from 0.030 to 0.050 $e^-/Å^3$ in solid lines.

discriminate between the three titled imidazobenzodiazepinones.

Experimental and Computational Methods

X-ray diffraction

Sarmazenil was crystallized by slow evaporation from a methylisobutylketone solution at room temperature. The crystals were colourless and prismatic.

Data were collected on a 4-circle diffractometer (CAD-4) with graphite monochromatized Cu (K_α,$\lambda = 1.54178$ Å). The unit cell parameters were obtained by least-squares refinement of the diffractometer settings for 25 medium order reflections. The measured intensities were corrected for Lorentz, polarization, and absorption effects. Further data collection details are provided in Table 1.

The structure was solved by the application of direct methods using SIR92.[51] The absorption correction was made by NRCVAX[52–57] and the structure refined by the method of full-matrix least-squares using NRCVAX[52–57] and SHELXL93.[58] Hydrogen atoms were calculated. Anisotropic temperature factors were used for all non-hydrogen atoms and isotropic ones were used for all hydrogen atoms. The final weighted least-squares cycle gave $R = 0.08$ with $w = 1.0/(s^2(F) + 0.002\ F^2)$. The geometric analysis was performed by PLATON92[59] and representation of the asymmetric unit and crystal packing by program ORTEP.[60]

Ab initio molecular orbital quantum calculations

Theoretical conformational calculations were performed using the semi-empirical quantum mechanical molecular orbital (MO) AM1 method developed by Dewar.[61] The good performance of this method for conformational analysis problems has been largely noted[61] and moreover, consideration of more sophisticated methods such as non-empirical ones would have been rather time consuming. The two-dimensional isoenergy contour maps were built by systematic variation (increment between two successive calculations: 15°) using the AM1 option with the standard parameters available within Gaussian92.[62] The generation of a 2-D isoenergy contour map taking account 625 conformations with AM1 takes ≈2 h of cpu time.

Molecular electronic properties were computed in the framework of the restricted Hartree–Fock–Roothan LCAO–MO–SCF formalism (Linear Combination of Atomic Orbitals – Molecular Orbitals – Self Consistent Field). Calculations were performed at the STO-3G* degree of sophistication of the LCAO expansion of the molecular orbitals as introduced by Collins.[63] Considering the relatively large dimensions of the current molecules (>22 heavy atoms), the minimal STO-3G* basis set was chosen as a cost-reliability compromise. Within this basis set, the computations included 124, 133, and 168 basic functions for flumazenil, sarmazenil, and bretazenil, respectively. A single geometry ab initio STO-3G* HF calculation takes ≈1 h; geometry optimizations take between 24 and 72 h. The atomic coordinates of the heavy atoms considered in the calculations were those obtained by crystallographic analysis. All H atoms were located at standard positions (distances, bond, and valence angles) from their carrier atoms.

Atomic charges and interatomic π-overlap percentages were calculated by the Mulliken charge population analysis.[64] The imidazole and phenyl rings were respectively placed in the xz plane, in order to differentiate the π electron contribution (i.e. the $2p_y$ component) from the total contribution.

The 3-D isopotential MEP maps were computed in a parallelipiped, surrounding each compound, which is run by a grid. The increment was fixed to 0.10 Å in planes parallel and perpendicular to the phenyl ring. The topologies of frontier orbitals were computed in a plan distant of 1.75 Å of the aromatic moieties of the molecules. This plane is run by a grid of points separated by 0.10 Å. Beside the wave function, the input consists in the desired molecular orbitals (all of them, or a particular desired one as the HOMO or LUMO) and their isoelectron charge density surface or contour values (from 0.005 to 0.050 electron/Å^3, step 0.005 electron/Å^3). The generation of the electron charge density isocontour maps was performed with the MOPLOT (Molecular Orbital PLOT) program.[65] The bielectronic integral cut-off and convergence on the density matrix threshold were fixed at 10^{-7} and 10^{-8}, respectively. Our experience has shown that within the basis set used, the computed total energy has at least seven significant digits. It corresponds to a numerical error of about 1 kcal/mol. The overlap populations (in electron) have four significant correct digits; only two digits are presented in the figures for clarity. The precision of the MEP values is 1 kcal/mol when taking into account points within grid separated by 0.10 Å. All 2-D and 3-D isopotential, isoenergy and isoelectron densities maps were drawn using the in-house device interactive contouring programs, CPS[66] and CPS3D,[67] developed in Fortran with the IBM graPHIGS Software.

Molecular graphics

The superimposition was performed with an in-house molecular modeling package, KEMIT,[68] developed with

the PHIGS standard for IBM RISC 6000 computer systems.

Conclusions

Several models of interaction of ligands with ω modulatory sites have been reported in the literature. These models were subsequently starting from the simple hypothesis (e.g. two site hypothesis of Fryer[69,70]) progressing towards complex models (e.g. Schove four-site model[47]) to a better understanding of ligand/receptor interaction. But all these models do not take into account the heterogeneity of the ω modulatory sites. In these studies, the parameters considered were successively π–π or charge transfer interaction, proton donor properties, steric and electrostatic interactions, proton accepting properties and finally relative distribution of the LUMO. The principal hypotheses of some of these models are abstracted hereafter.

The Fryer model[69,70] defined two sites that are required for recognition at the ω modulatory sites: a condensed aromatic ring and an electron-donating group. The distance between these sites was hypothesized to modulate intrinsic activity (agonist and antagonist). An additional electron-donating site was included for antagonists and inverse agonists.

The Codding–Muir model[71] consisted of three sites for receptor recognition: a condensed aromatic ring, a function involved in a π–π stacking interaction and a proton donor site. The two parameters modulating the intrinsic activities are a freely rotatable aromatic ring and an electron-withdrawing substituent on the condensed aromatic ring.

The Skolnick–Cook model[72,73] has been defined separately for agonists and antagonists/inverse agonists. Three sites of interaction are necessary for agonists: two hydrogen accepting atoms and a steric or electrostatic site. Only two sites are required for antagonists or inverse agonists: one hydrogen donor and one hydrogen acceptor site.

The Borea–Gilli model[74] postulated three proton accepting centers, two of which are necessary, involved in the receptor recognition. The authors postulate that different regions of the receptor cavity are occupied depending on drug structure that could change the conformation of the receptor.

The Tebib–Bourguignon-Wermuth model[75] showed three critical zones: a π-electron rich aromatic ring and two electron rich areas. Three other regions were defined as potential interaction sites like a freely rotating aromatic ring, an out-of-plane region strongly associated with agonism and a sterically sensitive area in the proximity of one of the electron rich zones, which leads to antagonism.

In the last model of Cook et al.,[76] three binding receptor sites are defined for the anchor of the ligands at the receptor. Only two of these sites and a lipophilic pocket are required for inverse agonist/antagonist activity. Agonist activity requires interactions with two hydrogen accepting atoms and two or three lipophilic pockets.

Recently, the Schove model[47] incorporates four important zones for receptor recognition: three binding receptor sites and a ring where the LUMO is centered and represents an electron accepting site. The authors proposed the distribution of the LUMO to be determinant for positive and negative allosteric modulation.

Most of the previous models were generated by studying a large number of heterogenous structures and the analysis of a limited number of parameters. In the present work, we focus our study on a large number of parameters but a limited number of chemical structures with the aim of fine-tuning the analysis of parameters, including molecular orbitals and proton affinities. Thus, with the goal of determining the structural and electronic properties governing the intrinsic activity of ligands for ω_1 modulatory sites, we have focused our study on three imidazobenzodiazepinone nonselective ligands with similar affinities for the ω_1 receptor subtype in order to limit the stereoelectronic dissimilarities due to chemical series heterogeneity. For the three molecules, crystal geometries, obtained by X-ray diffraction, were superimposed and reveal very similar spatial arrangement, except the orientation of the ester function which can be related with the intrinsic activity of the compounds. The comparison of the stereoelectronic descriptors used in this study have shown several features which could be responsible for recognition and activation at ω_1 modulatory sites and lead us to propose a five-site model for imidazobenzodiazepinone ligands-receptors interactions:

1. Three proton acceptor sites located at the imidazole nitrogen N_{13} atom and at the oxygen atoms of the lactam and the ester functions, that represent potential binding sites at the receptor. The nature and the conformation of the ester function as well as the proton affinity, calculated on relaxed molecules, appear to be discriminant for the molecules considered. The agonist properties of bretazenil at ω_1 modulatory sites could be a function of the orientation of the ester function and

the electron density at one of the proton acceptor sites of the molecule (the ester function). The stereoelectronic properties of sarmazenil are very close to those of the antagonist flumazenil according to the formerly described biological properties of this compound.

2. Two aromatic moieties, which could interact with the receptor: the LUMO of the electron acceptor phenyl ring and the HOMO of the electron donating imidazole ring. An additional π–π interaction involving the ester carbonyl group can be envisaged, as shown in the crystallographic packing of sarmazenil.

Future perspectives would consist of the development and refinement of a model of interaction for selective ω_1 ligands.

Acknowledgements

The authors are grateful to IBM-Belgium and the Facultés Universitaires Notre-Dame de la Paix Namur (FUNDP) for the use of the Namur Scientific Computing Facility and to the 'Fond National pour la Recherche Scientifique' (FNRS). B.L.R. thanks Mrs B. Norberg for technical assistance and Dr. J. G. Fripiat for his implementation of the Gaussian92 program on the IBM RISC platforms.

References and Notes

1. Zbinden, G.; Randall, L. O. *Adv. Pharmacol.* **1967**, *5*, 213.

2. *The Benzodiazepines: from Molecular Biology to Clinical Practice*; Costa, E., Ed.; Raven: New York, 1983.

3. Haefely, W. E. *Eur. Arch. Psychiatry Neurol. Sci.* **1989**, *238*, 294.

4. Haefely, W.; Polc, P.; Pieri, L.; Schaffner, R.; Laurent, J.-P. In *The Benzodiazepines: From Molecular Biology to Clinical Practice*; Costa, E., Ed.; Raven: New York, 1983; p 21.

5. Olsen, R. W. *Ann. Rev. Pharmacol. Toxicol.* **1982**, *22*, 245.

6. DeLorey, T. M.; Olsen, R. W. *J. Biol. Chem.* **1992**, *267*, 16747.

7. Hadingham, K. L.; Wingrove, P.; Le Bourdelles, B.; Palmer, K. J.; Ragan, C. I.; Whiting, P. *J. Mol. Pharmacol.* **1993**, *43*, 970.

8. Hadingham, K. L.; Wingrove, P. B.; Wafford, K. A.; Bain, C.; Kemp, J. A.; Palmer, K. J.; Wilson, A. W.; Wilcox, A. S.; Sikela, J. M.; Ragan, C. I.; Whiting, P. *J. Mol. Pharmacol.* **1993**, *44*, 1211.

9. Cutting, G. R.; Lu, L.; O'Hara, B. F.; Kasch, L. M.; Montrose-Rafizadeh, C.; Donovan, D. M.; Shimada, S.; Antonarakis, S. E.; Guggino, W. B.; Uhl, G. R.; Kazazian, Jr. H. H. *Proc. Natl. Acad. Sci. U.S.A.* **1991**, *88*, 2673.

10. Knoflach, F.; Rhyner, T.; Villa, M.; Kellenberger, S.; Drescher, U.; Malherbe, P.; Sigel, E.; Möhler, H. *FEBS Lett.* **1991**, *293*, 191.

11. Malherbe, P.; Sigel, E.; Baur, R.; Persohn, E.; Richards, J. G.; Möhler, H. *FEBS Lett.* **1990**, *260*, 261.

12. Ymer, S.; Draguhn, A.; Wisden, W.; Werner, P.; Keinänen, K.; Schofield, P. R.; Sprengel, R.; Pritchett, D. B.; Seeburg, P. H. *EMBO J.* **1990**, *9*, 3261.

13. Lüddens, H.; Pritchett, D. B.; Köhler, M.; Killisch, I.; Keinänen, K.; Monyer, H.; Sprengel, R.; Seeburg, P. H. *Nature* **1990**, *346*, 648.

14. Schofield, P. R.; Pritchett, D. B.; Sontheimer, H.; Kettenmann, H.; Seeburg, P. H. *FEBS Lett.* **1989**, *244*, 361.

15. Pritchett, D. B.; Sontheimer, H.; Shivers, B. D.; Ymer, S.; Kettenmann, H.; Schofield, P. R.; Seeburg, P. H. *Nature* **1989**, *338*, 582.

16. Ymer, S.; Schofield, P. R.; Draguhn, A.; Werner, P.; Köhler, M.; Seeburg, P. H. *EMBO J.* **1989**, *8*, 1665.

17. Khrestchatisky, M.; MacLennan, A. J.; Chiang, M.-Y.; Xu, W.; Jackson, M. B.; Brecha, N.; Sternini, C.; Olsen, R. W.; Tobin, A. J. *Neuron* **1989**, *3*, 745.

18. Shivers, B. D.; Killisch, I.; Sprengel, R.; Sontheimer, H.; Köhler, M.; Schofield, P. R.; Seeburg, P. H. *Neuron* **1989**, *3*, 327.

19. 1995 Receptor and Ion Channel Nomenclature Supplement, *Trends Pharmacol. Sci.* **1995**, 33.

20. Langer, S. Z.; Arbilla, S. *Pharmacol. Biochem. Behav.* **1988**, *29*, 763.

21. Dennis, T.; Dubois, A.; Benavides, J.; Scatton, B. *J. Pharmacol. Exp. Ther.* **1988**, *247*, 309.

22. Niddam, R.; Dubois, A.; Scatton, B.; Arbilla, S.; Langer, S. Z. *J. Neurochem.* **1987**, *49*, 890.

23. Doble, A.; Martin, I. L. *Trends Pharmacol. Sci.* **1992**, *13*, 76.

24. Wisden, W.; Laurie, D. J.; Monyer, H.; Seeburg, P. H. *J. Neurosci.* **1992**, *12*, 1040.

25. Laurie, D. J.; Seeburg, P. H.; Wisden, W. *J. Neurosci.* **1992**, *12*, 1063.

26. Braestrup, C.; Nielsen, M.; Honore, T.; Jensen, L. H.; Petersen, E. N. *Neuropharmacology* **1983**, *22*, 1451.

27. Haefely, W.; Kyburz, E.; Gerecke; M.; Möhler, H. *Adv. Drug Res.* **1985**, *14*, 165.

28. Julou, L.; Blanchard, J. C.; Dreyfus, J. F. *Pharmacol. Biochem. Behav.* **1985**, *23*, 653.

29. Arbilla, S.; Depoortere, H.; George, P.; Langer, S. Z. *Naunyn-Schmiedeberg's Arch. Pharmacol.* **1985**, *330*, 248.

30. Malatynska, E.; Serra, M.; Ikeda, M.; Biggio, G.; Yamamura, H. I. *Brain Res.* **1988**, *443*, 395.

31. Gardner, C. R.; Tully, W. R.; Hedgecock, C. J. R. *Prog. Neurobiol.* **1993**, *40*, 1.

32. Jensen, M. S.; Lambert, J. D. C. *Neurosci. Lett.* **1983**, *40*, 175.

33. Gardner, C. R. *Drug Dev. Res.* **1988**, *12*, 1.

34. Hunkeler, W.; Möhler, H.; Pieri, L.; Polc, P.; Bonetti, E. P.; Cumin, R.; Schaffner, R.; Haefely, W. *Nature* **1981**, *290*, 514.

35. Jensen, L. H.; Petersen, E. N.; Braestrup, C.; Honoré, T.; Kehr, W.; Stephens, D. N.; Schneider, H.. Seidelmann, D.; Schmiechen, R. *Psychopharmacology* **1984**, *83*, 249.

36. Valin, A.; Dodd, R. H.; Liston, D. R.; Potier, P.; Rossier, J. *Eur. J. Pharmacol.* **1982**, *85*, 93.

37. Cox, E. D.; Hagen, T. J.; Mckernan, R. M.; Cook, J. M. *Med. Chem. Res.* **1995**, *5*, 710.

38. Pike, V. W.; Halldin, C.; Crouzel, C.; Barré, L.; Nutt, D. J.; Osman, S.; Shah, F.; Turton, D. R.; Waters, S. L. *Nucl. Med. Biol.* **1993**, *20*, 503.

39. Tan, S.; Schoemaker, H. Synthelabo Recherche (L.E.R.S.), personal communication.

40. Puia, G.; Ducic, I.; Vicini, S.; Costa, E. *Proc. Natl. Acad. Sci. U.S.A.* **1992**, *89*, 3620.

41. Gath, I.; Weidenfeld, J.; Collins, G. I.; Hadad, H. *Br. J. Clin. Pharmacol.* **1984**, *18*, 541.

42. Nave, R.; Herer, P.; Lavie, P. *Psychopharmacology* **1994**, *115*, 366.

43. Nutt, D. J.; Lister, R. G. *Pharmacol. Biochem. Behav.* **1989**, *31*, 751.

44. Pieri, L.; Biry, P.; Wdonwicki, G. Br. *J. Pharmacol.* **1985**, *86*, 592P.

45. Allen, F. H.; Kennard, O. *Chem. Des. Automat. News* **1993**, *8*, 31.

46. Kyburz, E. *Il Farmaco* **1989**, *44*, 345.

47. Schove, L. T.; Perez, J. J.; Loew, G. H. *Bioorg. Med. Chem.* **1994**, *2*, 1029.

48. Ros, P. J. *Chem. Phys.* **1968**, *49*, 4902.

49. Del Bene, J. E.; Vaccaro, A. *J. Am. Chem. Soc.* **1976**, *98*, 7526.

50. Caronna, T.; Vittimberga, B. M. J. *Heterocyclic Chem.* **1992**, *29*, 787.

51. Altomare, A.; Cascarano, G.; Giacovazzo, C.; Guagliardi, A., SIR92, Ist. di Ric. per lo Sviluppo di Metodologie Cristallographiche, CNR, University of Bari, Italy, 1992.

52. Gabe, E. J.; Le Page, Y.; Charland,.J.-P.; Lee, F. L.; White, P. S. *J. Appl. Cryst.* **1989**, *22*, 384.

53. *International Tables for X-ray Crystallography*, Kynoch Press, Birmingham, England, 1974; Vol. IV.

54. Johnson, C. K., ORTEP—*A Fortran Thermal Ellipsoid Plot Program*, Technical Report ORNL-5138, Oak Ridge, 1976.

55. Motherwell S., PLUTO PLOTTING, *University Chemical Laboratory*, Cambridge, 1978.

56. Le Page, Y. *J. Appl. Cryst.* **1988**, *21*, 983.

57. Le Page, Y.; Gabe, E. J. *J. Appl. Cryst.* **1979**, *12*, 464.

58. Sheldrick, G. M. SHELXL93: *Program for the Refinement of Crystal Structures.* University of Göttingen:, Göttingen, Germany, 1993.

59. Spek, A. L. *Acta Crystallogr., Sect. A* **1990**, *46*, C3.

60. Johnson, C. K. ORTEP; Report ORNL-5138. Oak Ridge National Laboratory, Oak Ridge, TN, 1976.

61. Dewar, M. J. S.; Zoebisch, E. G.; Healy, E. F.; Stewart, J. P. P. *J. Am. Chem. Soc.* **1985**, *105*, 3902.

62. Frisch, M. J.; Trucks, G. W.; Head-Gordon, M.; Gill, P. M. W.; Wong, M. W.; Foresman, J. B.; Johnson, B. J.; Robb, M. A.; Replogle, E. S.; Gomperts, R.; Andres, J. L.; Raghavachari, K.; Binkley, J. S.; Gonzalez, C.; Martin, R. L.; Fox, D. J.; Defrees, D. J.; Baker, J.; Stewart, J. J. P.; Pople, J. A. *GAUSSIAN92*, rev 0.4. Gaussian, Pittsburgh, PA, 1992.

63. Collins, J.; Schleyer, P.; Binkley, J. S.; Pople, J. A. *J. Chem. Phys.* **1976**, *64*, 5142.

64. Mulliken, R. *J. Chem. Phys.* **1955**, *23*, 1833.

65. Hinde, R. J.; Luken, W. L.; Chin, S. *MOPLOT*; IBM Kingston Technical Report KGN-141; IBM: New York, NY, 1988.

66. Baudoux, G.; Vercauteren, D. P. *CPS, a Countering Plotting System*; Facultés Universitaires Notre-Dame de la Paix: Namur, Belgium, 1989.

67. Baudoux, G.; Dory, M.; Vercauteren, D. P. *CPS3D, Contour Monitoring System for Three-Dimensional Data*, Rel. 1; Facultés Universitaires Notre-Dame de la Paix, Namur, Belgium, 1993.

68. Vanderveken, D. J.; Vercauteren, D. P. *KEMIT, a Molecular Graphics System*, Rel 1.2; Facultés Universitaires Notre-Dame de la Paix: Namur, Belgium, 1989.

69. Fryer, R. I.; Cook, C.; Gilman, N. W.; Walser, A. *Life Sci.* **1986**, *39*, 1947.

70. Fryer, R. I. In *Comprehensive Medicinal Chemistry*, Hansch, C., Sammes, P. G., Taylor, J. B., Eds; Pergamon: Oxford, 1990; Vol. 3, p. 539.

71. Codding, P. W.; Muir, A. K. S. *Mol. Pharmacol.* **1985**, *28*, 178.

72. Allen, M. S.; Hagen, T. J.; Trudell, M. L.; Codding, P. W.; Skolnick, P.; Cook, J. M. *J. Med. Chem.* **1988**, *31*, 1854.

73. Hollinshead, S. P.; Trudell, M. L.; Skolnick, P.; Cook, J. M. *J. Med. Chem.* **1990**, *33*, 1062.

74. Borea, P. A.; Gilli, G.; Bertolasi, V.; Ferretti, V. *Mol. Pharmacol.* **1987**, *31*, 334.

75. Tebib, S.; Bourguignon, J. J.; Wermuth, C. G. *J. Comput. Aided Drug Design* **1987**, *1*, 153; (b) Zhang, W.; Köhler, K. F.; Zhang, P.; Cook, J. M. *Drug Des. Dis.* **1995**, *12*, 193.